

# Dynamic Programming Approximate Optimal Control for Model-Based Reinforcement Learning

Prakash Mallick<sup>1</sup>, Zhiyong Chen<sup>2</sup>

<sup>1</sup>Australian Institute of Machine Learning (AIML), <sup>2</sup>University of Newcastle

**Abstract**—This article proposes an improved trajectory optimization approach for stochastic optimal control of dynamical systems affected by measurement noise by combining optimal control with maximum likelihood techniques to improve the reduction of the cumulative cost-to-go. A modified optimization objective function that incorporates dynamic programming-based controller design is presented to handle the noise in the system and sensors. Empirical results demonstrate the effectiveness of the approach in reducing stochasticity and allowing for an intermediate step to switch optimization that can allow an efficient balance of exploration and exploitation mechanism for complex tasks by constraining policy parameters to parameters obtained as a result of this improved optimization. This research study also includes theoretical work on the uniqueness of control parameter estimates and also leverages a structure of the likelihood function which has an established theoretical guarantees. Furthermore, a theoretical result is also explored that bridge the gap between the proposed optimization objective function and existing information theory (relative entropy) and optimal control dualities.

**Index Terms**—Stochastic systems, optimal control, trajectory optimization, robust control, maximum likelihood, robust expectation maximization

## I. INTRODUCTION

Model-based trajectory optimization offers a general method of planning, and therefore has been utilized to generate/reproduce a wide range of behaviours; see e.g., [1], [2], [3]. However, such methods does not directly handle the partially observed environments. Research study conducted by [4] and [5] handled the latency in states fairly well over a 2D task; however these proposed paradigms have not been tested on more complicated tasks. This paper delves into empirical study of the expectation-maximization-based stochastic control approach widely evaluated on complicated robotic simulation framework assigned to carry out complex tasks. The new modified optimization approach leverages the fundamentals of dynamic programming and the newly formulated optimization routine has the same functional structure that of the likelihood. As a consequence of this, all of the theoretical results presented in the research studies of [4] can be leveraged into this newly proposed optimization procedure. The modified objective function is experimented on two complex tasks involving a PR2 similar robotic simulation platform i.e., MUJOCO [6]; details of which will be described later in the chapter.

The contributions of this research can be summarized as follows, with references to relevant works:

- The research methods developed in [4], [5] propose a sophisticated approach to address trajectory optimization, particularly in the presence of measurement noise. While Expectation-Maximization (EM) methods are effective in handling measurement noise, the simplicity and computational efficiency of iLQG [1] make it highly appealing for practical and industrial

Prakash Mallick is with the Australian Institute of Machine Learning (AIML) affiliated to University of Adelaide and Zhiyong Chen is with the School of Engineering, University of Newcastle, Callaghan, NSW 2308, Australia and Emails: prakash.mallick@adelaide.edu.au, zhiyong.chen@newcastle.edu.au

applications. Therefore, the subsequent sections of this chapter aim to integrate iLQG and EM-based stochastic optimal control (SOC) into a unified framework, which is evaluated on complex tasks.

- In order to introduce a novel dynamic programming-based optimization for locally optimal controller design, the optimization objective function has been modified. Building on the approach in [7], the locally optimal solutions of the newly proposed objective function guide the iLQG control design routine. The new policy is constrained by previous policies, and significant results are presented in the simulation experiments.
- Moreover, inspired by the research connection between information theory and optimal control dualities, particularly the work in [8], this study leverages these connections, with a focus on free energy [9]. The developed model can be interpreted as a special case of information theory (relative entropy) and optimal control dualities.
- Theoretical foundations establish the uniqueness characteristic of the maximizer of the likelihood function based on dynamic programming. This provides a practical and viable approach to achieve a lower-dimensional approximation in each iteration. Additionally, it is demonstrated that this new optimization technique effectively explores the state space, which is characterized by high uncertainty in the control actions of the robotic joints of the manipulator. Furthermore, numerical evidence showcases improved state trajectories with reduced stochasticity and better reduction in the cumulative cost-to-go.

The paper is organised in the following manner: Section II elucidates fundamental definitions of Kullback-Leibler divergence, relative entropy and free energy in a manner pertinent to the context of optimal control. Then, section II delineates the underlying mathematical problem statement, provides an explanation of the procedure of the solution. This is followed by Section IV, which demonstrates the new DP optimization and a few theoretical results which is new in accordance to the new objective function. Then, Section V of this manuscript focusses on providing an information theoretic view of the EM-based stochastic optimal control approach.

## II. PRELIMINARIES, PROBLEM STATEMENT AND SOLUTION PROCEDURE

In this section, the dynamic model being investigated, the problem formulation, and the proposed solvability procedure are presented. Additionally, the mathematical notations involved in addressing the problem discussed in this paper are elaborated upon. For a summary of the symbols used, readers may refer to Table I.

### A. Preliminaries

In this section, we briefly review the key concepts underlying the fundamental duality relationships between free energy and relative entropy [10]. Definition 1 presents the concept of “free energy”,

TABLE I: Summary of symbols

Symbol	Definition
$k, T$	Time instant, Length of episode
$\mathbf{s}_k$	Measured state (implementation) or latent state (optimization) at time instant $k$
$\mathbf{x}_k, \mathbf{a}_k$	Real state and control action at time instant $k$
$Y_k(\mathbf{s}_k, \mathbf{a}_k)$ or $Y_k(\mathbf{s}_k, \phi_k)$	Instantaneous cost at time instant $k$
$y_k$	Observed cost $p(Y_k)$
$\mathbb{S}_{T+1}$	Measured or latent variable $\{\mathbf{s}_1, \mathbf{s}_2, \dots, \mathbf{s}_{T+1}\}$
$\mathbb{Y}_T/\mathbb{A}_T$	Reward observation $\{y_1, y_2, y_3, \dots, y_T\}$ /Set of actions $\{\mathbf{a}_1, \mathbf{a}_2, \mathbf{a}_3, \dots, \mathbf{a}_T\}$
$\hat{\phi}^i$	Controller parameter $\phi$ at the $i$ -th iteration
$\mathbb{E}$	Expectation of a random variable
$V_\phi(\mathbb{S}_{T+1})$	Cumulative sum of expected costs
$L_\phi(\mathbb{Y}_T), \mathcal{L}(\phi, \hat{\phi}^i)$	Observation log-likelihood, Mixture likelihood
$\text{vec}(\cdot)$	Column vector stacked by vector of its matrix argument
$\text{col}(\dots)$	Column vector stacked by its column arguments
$\text{Tr}(\cdot)$	Trace of its matrix argument
$(\Omega, \mathcal{F})$	Sample space of an experiment, $\sigma$ -algebra respectively.
$\mathbf{P}(\Omega)$	probability measure on $\sigma$ -algebra $\mathcal{F}$
$\nabla, \nabla^2$	Gradient vector field, Hessian matrix; second-order partial derivative of a scalar function
$\top, \otimes$	Transpose operator, Kronecker product operator
$\mathbb{R} / \mathbb{R}^+$	Set of real numbers / positive numbers
$\mathbf{I}_{(s)}$	Identity matrix (of dimension $s$ )

involving measurable function and a probability measure on a measurable space. The free energy is defined as the expectation of the function under the probability measure, and it is obtained by taking the logarithm of the integral of the exponential of the function with respect to the probability measure. The function captures a state-dependent cost and includes a terminal cost as well as a sum of costs over a sequence of states. The parameter  $\rho$  determines a measure of risk associated with the free energy. Further details on this definition can be found in [9, Section 3].

Definition 2 introduces the notion of “relative entropy” or “Kullback-Leibler divergence”. It measures the difference between two probability measures, denoted as  $\mathbb{P}$  and  $\mathbb{Q}$ . The relative entropy of  $\mathbb{Q}$  with respect to  $\mathbb{P}$  is defined as an integral involving the logarithm of the ratio of the densities of  $\mathbb{Q}$  and  $\mathbb{P}$ . Further details and formal expressions can be found in [10]

**Definition 1.** Let the pair  $(\Omega, \mathcal{F})$  denote a measurable space<sup>1</sup>, where  $\Omega$  and  $\mathcal{F}$  corresponds to symbols mentioned in I, and let  $\mathbf{P}(\Omega)$  define a probability measure<sup>2</sup> on  $\sigma$ -algebra  $\mathcal{F}$ . Consider  $\mathbb{P} \in \mathbf{P}(\Omega)$  and the function  $\mathcal{J}(\cdot) : \mathcal{F} \rightarrow \mathbb{R}$  be a measurable function. Then the expectation term:

$$\mathbb{E}(\mathcal{J}(\mathbf{s}_k, k)) = \log \int e^{\rho \mathcal{J}(\mathbf{s}_k, k)} d\mathbb{P} \quad (1)$$

is called **free energy** of  $\mathcal{J}$  with respect to  $\mathbb{P}$ , where  $\mathcal{J}$  can be defined as,

$$\mathcal{J}(\cdot) \triangleq \mathcal{J}(\mathbf{s}_k, k) = g_T(\mathbf{s}_T) + \sum_{j=k}^{T-1} g_j(\mathbf{s}_j, \mathbf{w}_j) \quad (2)$$

a state dependent cost as described in [9, Section 3] and  $\mathbf{w}_k$  is a r.v. which corresponds to noise. The term  $\rho$  is a parameter which determines some measure of risk—please see [9], [8] for details.

**Definition 2.** Let  $\mathbb{P} \in \mathbf{P}(\Omega)$ , the **relative entropy** of  $\mathbb{P}$  with respect to  $\mathbb{Q}$  be defined as:

$$D_{KL}(\mathbb{Q}||\mathbb{P}) = \begin{cases} \int \log \frac{d\mathbb{Q}}{d\mathbb{P}} \mathbb{Q}, & \text{if } \mathbb{Q} \ll \mathbb{P} \text{ and } \log \frac{d\mathbb{Q}}{d\mathbb{P}} d\mathbb{Q} \in L^1. \\ +\infty, & \text{otherwise.} \end{cases} \quad (3)$$

<sup>1</sup>The definition of measurable space can be found [11, Page 160]

<sup>2</sup>Please refer to [11, Page 160]

The term  $L^1$  mentioned above describes functions on  $[0, \infty)$  integrable in the Lebesgue sense, and where “ $\ll$ ” denotes the absolute continuity of  $\mathbb{Q}$  with respect to  $\mathbb{P}$ . If one says that  $\mathbb{Q}$  is absolutely continuous with respect to  $\mathbb{P}$ , one can write  $\mathbb{Q} \ll \mathbb{P}$  if  $\mathbb{P}(H) = 0 \implies \mathbb{Q}(H) = 0, \forall H \in \mathcal{F}$ , where  $\mathcal{F}$  denotes a  $\sigma$ -algebra.

After having described few definitions, the next sub-section focuses on mathematical modelling of the dynamical systems, controller parameter, the objective function and a brief step-by-step procedure to attain the objective.

## B. Mathematical notation and modeling

The paper takes into account a stochastic dynamics that does not have a known model from first principles, in the presence of uncertainties such as parameter variation, external disturbance, sensor noise, etc. The completed system is considered to be a global model,  $O$ , that is composed of multiple local models  $o^l, l = \{1, 2, \dots\}$ , and each of which follows an MDP, called a local model. We are interested in a finite-horizon optimal control for a particular initial state, rather than for all possible initial states. The procedure to handle numerous initial states is laid out in [5] which utilizes the policy structure of this paper to generalize to numerous initial conditions.

The partially observable MDP encompasses a *latent state*  $\mathbf{s}_k \in \mathbb{R}^{n_s}$  and a *control action*  $\mathbf{a}_k \in \mathbb{R}^{n_a}$ , at time instant  $k = 1, 2, \dots$ , and the local state transition dynamic model is represented by a conditional probability density function (p.d.f.) expressed as:

$$p(\mathbf{s}_{k+1} | \mathbf{s}_k, \mathbf{a}_k). \quad (4)$$

In particular, for  $k = 1, \mathbf{s}_1 \in \mathbb{R}^{n_s}$  is called the *initial state*, obeying a specified distribution. Variables  $n_s$  and  $n_a$  are integers which are the dimensions of state and action space. We specifically consider a finite-horizon MDP in this paper for  $k = 1, 2, \dots, T$ , called an *episode*, with the time instant  $T$  being the end of episode. It is worth mentioning that the p.d.f. in (4) varies with time  $k$  and the time-varying nature is capable of characterizing more complicated dynamical behaviors but also brings more challenges in control design. It will be elaborated in Section IV.

The entity  $Y_k(\mathbf{s}_k, \mathbf{a}_k) \in \mathbb{R}^+$  denotes the instantaneous real valued cost for executing action  $\mathbf{a}_k$  at state  $\mathbf{s}_k$ . It has a more specific expression as follows,

$$Y_k(\mathbf{s}_k, \mathbf{a}_k) = (\mathbf{s}_k - \mathbf{s}^*)^\top \mathbf{Q}_s (\mathbf{s}_k - \mathbf{s}^*) + (\mathbf{a}_k - \mathbf{a}^*)^\top \mathbf{Q}_a (\mathbf{a}_k - \mathbf{a}^*), \quad (5)$$

where  $\mathbf{s}^*$  and  $\mathbf{a}^*$  are the target state and control action, respectively, and  $\mathbf{Q}_s > 0$  and  $\mathbf{Q}_a > 0$  are some specified matrices. As  $\mathbf{s}_k$  and  $\mathbf{a}_k$  are random variables,  $Y_k(\mathbf{s}_k, \mathbf{a}_k)$  (with  $Y_k$  a continuous and deterministic function) is also a random variable, shorted as  $Y_k$ . We develop another variable, i.e.,  $y_k = F(Y_k) \in \mathbb{R}^+$  (known as *observed cost*) which is the exponential transformation of the immediate cost  $Y_k(\mathbf{s}_k, \mathbf{a}_k)$  following a p.d.f.  $p(y_k | \mathbf{s}_k, \mathbf{a}_k)$ , which will be elaborated later.

Overall, the MPD consists of the transition dynamics  $p(\mathbf{s}_{k+1} | \mathbf{s}_k, \mathbf{a}_k)$  and the cost observation p.d.f.  $p(y_k | \mathbf{s}_k, \mathbf{a}_k)$  in an augmented form, i.e.,

$$p\left(\begin{bmatrix} \mathbf{s}_{k+1} \\ y_k \end{bmatrix} | \mathbf{s}_k, \mathbf{a}_k\right) = \mathcal{N}\left(\begin{bmatrix} \mathbf{s}_k \\ \mathbf{a}_k \end{bmatrix}, \Sigma_k^o\right), \quad (6)$$

which is referred to as the *dynamic model* in the subsequent parts of the paper. The symbol  $\mathcal{N}(\cdot, \cdot)$  is used to denote a Gaussian distribution with the two parameters of mean and variance. A time-varying linear Gaussian p.d.f. is used in (6) as an approximation of a real model which is in general nonlinear, where the matrices  $\mathbf{A}_k^o$  and  $\Sigma_k^o$  is to be determined in Section III using the dynamic model fitting technique.



state  $\mathbf{s}_k$  is physically measured, which represents the observed system state carrying measurement noise. However, in Steps 2 and 3, only theoretical computation is conducted without operating the real system, thus leveraging the latency nature of states. In this context,  $\mathbf{s}_k$  represents the explored state obeying a joint probability  $p_\phi(\mathbb{S}_{T+1}|\mathbb{Y}_T)$  and contains noise. Thus, the actual or true system states remain unobserved, and the model described in Equation (6) is treated as a partially observable Markov decision process (POMDP). In Step 4, a DDP-based optimal control design is employed while constraining the policy derived from Step 3.

The subsequent sections are concerned with the optimization problem (12), which is regarded as the approximation of the original optimization problem (10). It is easy to see that (12) is equivalent to

$$\min_{\mathbf{a}_1, \mathbf{a}_2, \dots, \mathbf{a}_T} \mathbb{E}_{p_\phi(\mathbb{S}_{T+1}|\mathbb{Y}_T)} \sum_{k=1}^T Y_k(\mathbf{s}_k, \mathbf{a}_k). \quad (14)$$

It is expected that recursively solving the problem (12) or (14) will approach a solution to (10). However, the global convergence is a great challenge and the effectiveness can only be numerically/empirically verified. The next section describes the new optimization approach.

### III. DYNAMICS FITTING

In this section, the authors first provide a specific definition of  $y_k$  and an expression of its density function. Additionally, they provide a detailed explanation of the procedure formulated in Step 1 for obtaining linear time-varying parameter estimates of the dynamic model represented by equation (6). This procedure combines the methodology employed in [23] with existing variational Bayesian (VB) strategies used for a finite mixture model, as outlined in [24].

A specific definition of the variable  $y_k$  is presented as follows:

$$y_k(\mathbf{s}_k, \mathbf{a}_k) = e^{-Y_k(\mathbf{s}_k, \mathbf{a}_k)}. \quad (15)$$

The variable  $y_k(\mathbf{s}_k, \mathbf{a}_k)$ , which takes values in the interval  $(0, 1]$ , characterizes the likelihood of the state-action pair  $(\mathbf{s}_k, \mathbf{a}_k)$  being in proximity to the optimal trajectory. A lower cost value  $Y_k(\mathbf{s}_k, \mathbf{a}_k)$  corresponds to a higher value of  $y_k(\mathbf{s}_k, \mathbf{a}_k)$ , indicating an increased likelihood of proximity to the optimal trajectory. The exponential transformation has been demonstrated to be successful in determining the probability of an optimal event occurring in optimal control, as evidenced by previous studies such as [25].

The following is an assumption for the p.d.f. of  $Y_k$ .

**Assumption III.1.** *The p.d.f. of  $Y_k$  follows an exponential distribution with parameter  $\lambda$ , i.e.,*

$$p(Y_k) = \lambda e^{-\lambda Y_k} \text{ where } \lambda > 1. \quad (16)$$

The use of an exponential distribution is supported by relevant work. For instance, [26] assumes rewards (negative costs) are sampled from an exponential distribution, while [27] utilizes an exponentiated payoff distribution to establish a connection between maximum likelihood and an optimal control objective.

**Lemma III.1.** *For  $Y_k$  of the p.d.f. (16), the random variable  $y_k$  in (15) has a p.d.f. of the form*

$$p(y_k) = \lambda y_k^{\lambda-1}. \quad (17)$$

**Proof.** Please see [4].  $\square$

One can run one iteration of experiment and collect tuples of measured  $\{\mathbf{x}_k, \mathbf{u}_k, \mathbf{x}_{k+1}, y_k\}$  for one episode  $k = 1, \dots, T$ . Practically, one can repeat the experiments for  $M$  times from the same initial

conditions with a random seed value to gather sufficiently many samples, each of which is denoted by

$$\mathcal{D}_k^m = \{\mathbf{x}_k, \mathbf{u}_k, \mathbf{x}_{k+1}, y_k\}_{m\text{-th experiment}},$$

for  $m = 1, \dots, M$ . Let  $\mathcal{D}_k = \{\mathcal{D}_k^1, \dots, \mathcal{D}_k^M\}$  and  $\mathcal{D} = \{\mathcal{D}_1, \dots, \mathcal{D}_T\}$ . Then, one can fit a Gaussian mixture model (GMM) to the data set  $\mathcal{D}$ . In particular, the VB inference method is used to determine the parameters of the GMM, i.e., the means, covariances and weights of the Gaussians.

The GMM produced as a result of VB inference acts as a considerable global prior and it helps in bringing in information to construct a solitary normal-inverse Wishart (NIW) distribution. This NIW acts as a conjugate prior for a Gaussian distribution

$$p(\mathbf{x}_k, \mathbf{u}_k, \mathbf{x}_{k+1}, y_k) = \mathcal{N}(\boldsymbol{\mu}_k, \boldsymbol{\Lambda}_k). \quad (18)$$

Next, it will be elaborated that the NIW prior plays an essential role in attaining the parameters, i.e., the mean  $\boldsymbol{\mu}_k$  and the covariance  $\boldsymbol{\Lambda}_k$ .

The procedure of fitting GMM to  $\mathcal{D}$  involves constructing NIW distributions to act as prior for means and covariances of Gaussian distributions involved in mixture model. In addition to it, Dirichlet distributions are defined to be the prior on the weights of the Gaussian distributions which would explain the mixing proportions of Gaussians. Then, iterative VB strategy is adopted to increase the likelihood of joint variational distribution (see e.g., [24]-Section 10.2) for attaining the parameters of GMM. The attained parameters of GMM are utilized to further obtain the parameters of the solitary NIW prior which acts a representative of the global GMM prior. The purpose of NIW prior is to garner the information contained in the global GMM prior. The mean of the solitary NIW prior is  $\boldsymbol{\mu}_k^0 = \sum_{c=1}^C (w_k^c \boldsymbol{\mu}_k^c)$  where  $w_k^c$  and  $\boldsymbol{\mu}_k^c$  are the weight and mean of the  $c$ -th Gaussian in the GMM and  $C$  is the total number of initialized Gaussian clusters. The precision matrix  $\boldsymbol{\Lambda}_k^0$  of the solo NIW prior is evaluated by calculating the deviation of each cluster from  $\boldsymbol{\mu}_k^0$ . There are two more essential parameters of the solo NIW conjugate prior namely  $n_0$  and  $k_0$ , which are set for the total  $M$  samples. Define the empirical mean,  $\boldsymbol{\mu}_k^{emp} \in \mathbb{R}^{n_u+2n_x+1}$  and the covariance  $\boldsymbol{\Lambda}_k^{emp} \in \mathbb{R}^{(n_u+2n_x+1) \times (n_u+2n_x+1)}$  as follows, for the data set  $\mathcal{D}_k$ ,

$$\boldsymbol{\mu}_k^{emp} = \frac{1}{M} \sum_{m=1}^M \mathcal{D}_k^m \ \& \ \boldsymbol{\Lambda}_k^{emp} = \frac{1}{M} \sum_{m=1}^M (\mathcal{D}_k^m - \boldsymbol{\mu}_k^{emp})(\mathcal{D}_k^m - \boldsymbol{\mu}_k^{emp})^\top. \quad (19)$$

Next, one can carry out Bayesian update that results in a-posteriori estimates of the mean and precision matrix for the solo Gaussian in (18), that is,

$$\boldsymbol{\mu}_k = \frac{k_0 \boldsymbol{\mu}_k^0 + M \boldsymbol{\mu}_k^{emp}}{k_0 + M}, \ \boldsymbol{\Lambda}_k = \frac{(\boldsymbol{\Lambda}_k^0)^{-1} + M \cdot \boldsymbol{\Lambda}_k^{emp} + \boldsymbol{\kappa}_k}{M + n_0} \quad (20)$$

where  $\boldsymbol{\kappa}_k = [k_0 M / (k_0 + M)] (\boldsymbol{\mu}_k^{emp} - \boldsymbol{\mu}_k^0)(\boldsymbol{\mu}_k^{emp} - \boldsymbol{\mu}_k^0)^\top$ .

The Gaussian distribution (18) can be conditioned on states and action, i.e.,  $(\mathbf{x}_k, \mathbf{u}_k)$ , using standard identities of multivariate Gaussians, which delivers the following parameters of (6) i.e.,

$$\mathbf{A}_k^P = \begin{bmatrix} \mathbf{A}_k^d & \mathbf{B}_k^d \\ \mathbf{A}_k^y & \mathbf{B}_k^y \end{bmatrix}, \ \boldsymbol{\Sigma}_k^P = \begin{bmatrix} \boldsymbol{\Sigma}_k^{d\top} & \boldsymbol{\Sigma}_k^{yd} \\ \boldsymbol{\Sigma}_k^{yd\top} & \boldsymbol{\Sigma}_k^y \end{bmatrix}.$$

The dimensions of the matrices are  $\mathbf{A}_k^d \in \mathbb{R}^{n_s \times n_s}$ ,  $\mathbf{B}_k^d \in \mathbb{R}^{n_s \times n_a}$ ,  $\boldsymbol{\Sigma}_k^d \in \mathbb{R}^{n_s \times n_s}$ ,  $\mathbf{A}_k^y \in \mathbb{R}^{1 \times n_s}$ ,  $\mathbf{B}_k^y \in \mathbb{R}^{1 \times n_a}$ ,  $\boldsymbol{\Sigma}_k^y \in \mathbb{R}$ ,  $\mathbf{A}_k^P \in \mathbb{R}^{(n_s+1) \times (n_s+n_a)}$  and  $\boldsymbol{\Sigma}_k^P \in \mathbb{R}^{(n_s+1) \times (n_s+1)}$ .

### IV. DP OPTIMIZATION OF MIXTURE LIKELIHOOD

This section describes the details of the expression of the objective function which will be optimized, two theoretical results which are obtained by taking a similar approach to that of [4].

---

**Algorithm 1** DPSOC-EM algorithm
 

---

- 1: **Initialization:** Set  $i = 0$  and initialize  $\hat{\phi}^0$  from one of the baselines (iLQG).
  - 2: Run the real system under the controller (7) with the controller parameter vector  $\hat{\phi}^i$  to collect the data set  $\mathcal{D}$ ;
  - 3: Identify the dynamic model (6) by fitting it to  $\mathcal{D}$  via VB inference.
  - 4: Generate the cost observations  $\mathbb{Y}_T$  using the dynamic model (6) and the controller (7) with the controller parameter vector  $\hat{\phi}^i$ .
  - 5: Perform the Kalman filter and R.T.S. smoother recursions to evaluate (35) and hence  $\bar{\mathcal{L}}_k(\phi_k, \hat{\phi}^i)$ ,  $k = 1, \dots, T$ .
  - 6: Find  $\hat{\phi}_j^{i*}$ ,  $j = T, \dots, 1$  according to (32).
  - 7: Update  $\hat{\phi}^{i+1} = \hat{\phi}^{i*}$ .
  - 8: **if**  $i + 1 < \text{number of recursions}$  **then**
  - 9:   Let  $i = i + 1$ ; go to 2.
  - 10: **else**
  - 11:   Generate DDP solutions  $\pi_{\phi_1}, \dots, \pi_{\phi_n}$
  - 12:   Build initial sample set  $S$  from  $\pi_{\phi_1}, \dots, \pi_{\phi_n}, \pi_{\hat{\phi}^{i+1}}$
  - 13:   **for** number of iterations of iLQG  $g \in \{0, \dots, G\}$  **do**
  - 14:     Choose current sample set  $S_g \subset S$
  - 15:     Optimize  $\phi = \min_{\phi} \mathbb{E}_{p_{\phi}} [Q(\mathbf{s}_k, \mathbf{a}_k)]$  s.t.  $D_{KL}(p_{\phi} || p_{\hat{\phi}^{i+1}}) \leq \nu_k$  as per [28, Section 3.1]
  - 16:     Append samples from  $\pi_{\phi}$  to  $S_g$ .
  - 17:   **end for**
  - 18: **end if**
  - 19: Return the best policy  $\pi_{\phi}$ .
- 

### A. Composite expression of mixture likelihood

This section introduces key concepts related to the widely recognized EM algorithm. The EM algorithm aims to estimate the parameter vector  $\phi$  (which is customizable by the user) that maximizes the likelihood of an observed data set  $\mathbb{Y}_T$ . Specifically, the likelihood of observing the data, denoted as  $p_{\phi}(\mathbb{Y}_T)$ , is iteratively maximized during the algorithm's execution as per,

$$\hat{\phi}_{EM} \in \{\phi \in \Phi : p_{\phi}(\mathbb{Y}_T) \geq p_{\hat{\phi}^i}(\mathbb{Y}_T)\}, \quad (21)$$

where  $\hat{\phi}^i$  is a (known) considerably good parameter estimate with which the EM approach is initialized (at the iteration labeled  $i$ ).

The algorithm ensures that the estimate  $\hat{\phi}_{EM}$  satisfies the condition expressed by Equation 21, where  $\hat{\phi}^i$  represents a known and reasonably accurate initial parameter estimate at iteration  $i$ . This condition guarantees that the likelihood of the data  $p_{\phi}(\mathbb{Y}_T)$  is not lower than the likelihood associated with  $\hat{\phi}^i$ .

The EM algorithm involves the computation of the *observation log-likelihood* denoted as  $L_{\phi}(\mathbb{Y}_T)$ , as defined in eq. 22. Additionally, it approximates the logarithm of the *mixture likelihood* of latent variables ( $S_{T+1}$ ) and observations ( $\mathbb{Y}_T$ ) using a surrogate function denoted as  $\mathcal{L}(\phi, \hat{\phi}^i)$ , defined in Equation 23.

It is assumed that both  $L_{\phi}(\mathbb{Y}_T)$  and  $\mathcal{L}(\phi, \hat{\phi}^i)$  are differentiable with respect to  $\phi \in \Phi$ .

$$L_{\phi}(\mathbb{Y}_T) \triangleq \log p_{\phi}(\mathbb{Y}_T) \quad (22)$$

$$\mathcal{L}(\phi, \hat{\phi}^i) \triangleq \mathbb{E}_{\hat{\phi}^i}(\log p_{\phi}(S_{T+1}, \mathbb{Y}_T) | \mathbb{Y}_T). \quad (23)$$

Next, the primary objective is to maximize the mixture likelihood  $\mathcal{L}(\phi, \hat{\phi}^i)$ . The proposed optimization approach aims to find an improved policy parameter  $\phi = \hat{\phi}^{i+1}$  for the next iteration that

maximizes (or increases)  $\mathcal{L}(\phi, \hat{\phi}^i)$  compared to  $\phi = \hat{\phi}^i$ . This will be done as per,

$$\hat{\phi}^{i*} = \arg \max_{\phi} \mathcal{L}(\phi, \hat{\phi}^i). \quad (24)$$

So, it is ideal to select  $\hat{\phi}^{i+1} = \hat{\phi}^{i*}$ . The explicit expression of the mixture likelihood  $\mathcal{L}(\phi, \hat{\phi}^i)$  and a result presenting a connection between mixture likelihood and cumulative sum of cost-to-go mentioned in eq (10) is given in Lemma IV.1 and IV.2 respectively. These results are adopted from [4] and are utilized to introduce an alternative approximate optimization framework that capitalizes on the underlying principles of the principle of optimality (refer to [29, Section 1.3]). By employing this approach, optimal estimates of the control policy can be attained. A detailed description of the proposition, which relies on the principle of optimality, can be found in Proposition IV.1.

**Lemma IV.1.** *The expression for the function  $\mathcal{L}(\phi, \hat{\phi}^i)$  considering the dynamic model (6) and the controller (6) is given by:*

$$\mathcal{L}(\phi, \hat{\phi}^i) = \log p(\mathbf{s}_1) + \sum_{k=1}^T \bar{\mathcal{L}}_k(\phi_k, \hat{\phi}^i), \quad (25)$$

for

$$\begin{aligned} \log p(\mathbf{s}_1) &= -\frac{1}{2} \log |\mathbf{P}_1| + (\mathbf{s}_1 - \boldsymbol{\mu}_1)^{\top} \mathbf{P}_1^{-1} (\mathbf{s}_1 - \boldsymbol{\mu}_1), \\ \bar{\mathcal{L}}_k(\phi_k, \hat{\phi}^i) &= -\frac{1}{2} \text{Tr} \{ \boldsymbol{\Sigma}_k^{\phi-1} (\mathbb{E}_{\hat{\phi}^i}(\boldsymbol{\zeta}_k \boldsymbol{\zeta}_k^{\top} | \mathbb{Y}_T) - \mathbb{E}_{\hat{\phi}^i}(\boldsymbol{\zeta}_k \mathbf{z}_k^{\top} | \mathbb{Y}_T) \mathbf{A}_k^{\phi \top} \\ &\quad - \mathbf{A}_k^{\phi} [\mathbb{E}_{\hat{\phi}^i}(\boldsymbol{\zeta}_k \mathbf{z}_k^{\top} | \mathbb{Y}_T)]^{\top} + \mathbf{A}_k^{\phi} \mathbb{E}_{\hat{\phi}^i}(\mathbf{z}_k \mathbf{z}_k^{\top} | \mathbb{Y}_T) \mathbf{A}_k^{\phi \top}) \} - \frac{1}{2} \log |\boldsymbol{\Sigma}_k^{\phi}|, \end{aligned} \quad (26)$$

where initial state  $\mathbf{s}_1$  follows a Gaussian distribution with some known mean  $\boldsymbol{\mu}_1$  and covariance  $\mathbf{P}_1$  and  $\boldsymbol{\zeta}_k = \text{col}(\mathbf{s}_{k+1}, y_k)$  and  $\mathbf{z}_k = \text{col}(\mathbf{s}_k, \mathbf{a}_k)$ .

**Lemma IV.2** (Theorem IV.1 of [4]). *Suppose the parameter  $\hat{\phi}^{i+1}$  is produced such that*

$$\mathcal{L}(\hat{\phi}^{i+1}, \hat{\phi}^i) \geq \mathcal{L}(\hat{\phi}^i, \hat{\phi}^i). \quad (27)$$

Then, the cumulative sum of expected costs defined in (9) satisfies

$$\mathbb{E}_{\hat{\phi}^i}(V_{\hat{\phi}^{i+1}}(S_{T+1}) | \mathbb{Y}_T) \leq \mathbb{E}_{\hat{\phi}^i}(V_{\hat{\phi}^i}(S_{T+1}) | \mathbb{Y}_T). \quad (28)$$

**Proposition IV.1.** *For an initial state  $s_1$ , the optimal likelihood function  $\mathcal{L}^*(s_1) \triangleq \mathcal{L}(\hat{\phi}^*, \hat{\phi}^i)$  of the above-mentioned problem (i.e., eq (24)) is given by the last step of the following algorithm, which proceeds backwards in time from period  $T$  to period 1. Therefore, the optimal parameters are obtained as a consequence of sequentially maximizing the likelihood backwards as presented in the following equations,*

$$\hat{\phi}_T^{i*} = \arg \max_{\phi_T} \bar{\mathcal{L}}_T(\phi_T, \hat{\phi}^i) \quad (29)$$

$$\hat{\phi}_{T-1}^{i*} = \arg \max_{\phi_{T-1}} \bar{\mathcal{L}}_{T-1}(\phi_{T-1}, \hat{\phi}^i) + \bar{\mathcal{L}}_T(\hat{\phi}_T^{i*}, \hat{\phi}^i) \quad (30)$$

$$\vdots \quad (31)$$

$$\hat{\phi}_j^{i*} = \arg \max_{\phi_j} \bar{\mathcal{L}}_j(\phi_j, \hat{\phi}^i) + \sum_{k=j+1}^T \bar{\mathcal{L}}_k(\hat{\phi}_k^{i*}, \hat{\phi}^i), \quad j = T, \dots, 2 \quad (32)$$

where  $\bar{\mathcal{L}}_k(\phi_k, \hat{\phi}^i)$  is defined as in (26) and the expectation inside each of the terms is taken with respect to the measurement states which are a result of instantiations of the noise in the dynamical equation. In addition to that, if  $\mathbf{a}_k^*$  maximizes the term on the right in eq (32) for each  $\mathbf{s}_k$  and  $k$ , the policy  $\pi^* = \{\mathbf{a}_1^*, \dots, \mathbf{a}_T^*\}$  is optimal.

**Remark IV.1.** *Precisely, there are two main reasons for proposing optimization according to eq (32),*

- *Lemma IV.2 establishes connections that likelihoods can be treated as costs with certain assumptions and approximations. Therefore, one can intuitively think of optimizing the approximate likelihood function from the last time step backwards in time in a very similar manner to that of the principle of optimality [29].*
- *The variance of the estimators of  $\phi_j$  can be reduced by utilizing the fact that the calculation of future optimal parameters of actions mentioned in (32) does not take into account past likelihood functions unlike the objective function mentioned in [4, Section V-B].*

Attention is now directed towards the resolution of equation (32). The proposed optimization paradigm aims to identify a superior policy parameter  $\phi = \hat{\phi}^{i+1}$  for the next iteration compared to  $\phi = \hat{\phi}^i$ , with the objective of maximizing (or increasing) the right-hand side of equation (32). Hence, it is desirable to choose  $\hat{\phi}^{i+1} = \hat{\phi}^{i*}$ .

Nevertheless, computing the optimal value of  $\hat{\phi}^{i*}$  across the entire control action sequence  $\mathbf{a}_1, \mathbf{a}_2, \dots, \mathbf{a}_T$  is typically challenging. The principle of expectation-maximization (EM) as an optimal control technique simplifies the maximization of  $\mathcal{L}(\phi, \hat{\phi}^i)$  over the entire control action sequence for each time step. In other words, one aims to maximize  $\mathcal{L}(\phi, \hat{\phi}^i)$  individually for each time step through a backward iterative process, as indicated by equations (29)-(32) for  $j = T, \dots, 1$ .

Then, a better policy parameter for the next iteration is selected as  $\hat{\phi}^{i+1} = \text{col}(\hat{\phi}_1^{i*}, \dots, \hat{\phi}_T^{i*}) \approx \hat{\phi}^{i*}$ . For brevity we would refer the above optimization problem as **DPSOC-EM**. After carrying out the maximization, we utilize the optimal parameters to collect samples of trajectories, that are utilized to carry out the dynamics fitting of piecewise linear models according to the procedure mentioned in [5]. Then, with the help of those dynamics I carry out another degree of optimization as per:

$$\phi = \min_{\phi} \mathbb{E}_{p_{\phi}} [Q(s_k, \mathbf{a}_k)] \text{ s.t. } D_{KL}(p_{\phi} || p_{\hat{\phi}^{i+1}}) < v_k \quad (33)$$

where  $Q(s_k, a_k)$  is a second-order Taylor series expansion employed around the nominal state-action pair  $(\hat{s}_k, \hat{\mathbf{a}}_k)$  as mentioned in [17, Chapter 3.4]. The term  $p_{\hat{\phi}^{i+1}}$  in eq (33) denotes the distribution of policy when excited with parameters  $\hat{\phi}^{i+1}$ . The term  $v_k$  is the maximum Kullback-Leibler divergence between the new policy and the EM policy parameterized with  $\hat{\phi}^{i+1}$ . More details can be found in [28], [30].

Having, described the new proposition, I present two results described in Theorem IV.1 and IV.2 that delivers some properties of the optimal estimates of **DPSOC-EM**.

**Theorem IV.1.** *The following equation,*

$$\nabla_{\phi_j} \left\{ \bar{\mathcal{L}}_j(\phi_j, \hat{\phi}^i) + \sum_{k=j}^T \bar{\mathcal{L}}_k(\hat{\phi}_{j+1}^*, \hat{\phi}^i) \right\} = \mathbf{0}, \quad j = T, \dots, 1 \quad (34)$$

*has a unique solution for any given parameter  $\hat{\phi}^i$  for the function  $\bar{\mathcal{L}}_k(\phi_k, \hat{\phi}^i)$  defined in (26)*

**Proof.** The function  $\bar{\mathcal{L}}_k(\phi_j, \hat{\phi}^i)$  defined in (34) is expressed in terms of

$$\mathbb{E}_{\hat{\phi}^i}(y_k y_k^{\top} | \mathbb{Y}_T), \mathbb{E}_{\hat{\phi}^i}(\mathbf{a}_k \mathbf{a}_k^{\top} | \mathbb{Y}_T), \mathbb{E}_{\hat{\phi}^i}(y_k \mathbf{a}_k^{\top} | \mathbb{Y}_T), \quad (35)$$

where  $\mathbf{a}_k$  explicitly depends on  $\phi_k$ . Now, one can take a very similar approach as that of [4, Theorem IV.1] to prove the following theorem,

where components of expression of Jacobian can be described as follows,

$$\nabla_{\phi_j} \left\{ \bar{\mathcal{L}}_j(\phi_j, \hat{\phi}^i) + \sum_{k=j}^T \bar{\mathcal{L}}_k(\hat{\phi}_{j+1}^*, \hat{\phi}^i) \right\} = \nabla_{\phi_j} \text{Tr} \boldsymbol{\lambda}_k + \boldsymbol{\mathcal{C}}^{\top} \quad (36)$$

where

$$\boldsymbol{\lambda}_k = \boldsymbol{\Sigma}_k^{d-1} \mathbf{B}_k^d \mathbb{E}_{\hat{\phi}^i}(\mathbf{a}_k \mathbf{a}_k^{\top} | \mathbb{Y}_T) \mathbf{B}_k^{d\top} \quad (37)$$

and  $\boldsymbol{\mathcal{C}}$  represents some constant column vector, independent of  $\phi_j = \text{col}(\mathbf{f}_j, \mathbf{e}_j, \boldsymbol{\sigma}_j)$ . In particular, one has  $\boldsymbol{\lambda}_k = \boldsymbol{\lambda}_{1,k} + \boldsymbol{\lambda}_{2,k} + \boldsymbol{\lambda}_{3,k} + \boldsymbol{\lambda}_{4,k} + \boldsymbol{\lambda}_{5,k}$  with

$$\begin{aligned} \boldsymbol{\lambda}_{1,k} &= (\boldsymbol{\Sigma}_k^d)^{-1} \mathbf{B}_k^d \mathbf{F}_j \mathbf{G}_k \mathbf{F}_j^{\top} \mathbf{B}_k^{d\top} \\ \boldsymbol{\lambda}_{2,k} &= (\boldsymbol{\Sigma}_k^d)^{-1} \mathbf{B}_k^d \mathbf{e}_j \mathbf{e}_j^{\top} \mathbf{B}_k^{d\top} \\ \boldsymbol{\lambda}_{3,k} &= (\boldsymbol{\Sigma}_k^d)^{-1} \mathbf{B}_k^d \boldsymbol{\Sigma}_j \mathbf{B}_k^{d\top} \\ \boldsymbol{\lambda}_{4,k} &= (\boldsymbol{\Sigma}_k^d)^{-1} \mathbf{B}_k^d \mathbf{F}_j \hat{\mathbf{s}}_{k|T} \mathbf{e}_j^{\top} \mathbf{B}_k^{d\top} \\ \boldsymbol{\lambda}_{5,k} &= (\boldsymbol{\Sigma}_k^d)^{-1} \mathbf{B}_k^d \mathbf{e}_j \hat{\mathbf{s}}_{k|T}^{\top} \mathbf{F}_j^{\top} \mathbf{B}_k^{d\top}. \end{aligned}$$

Also,  $\boldsymbol{\mathcal{C}}$  is of the special structure

$$\boldsymbol{\mathcal{C}} = \begin{bmatrix} \sum_{k=j}^T \boldsymbol{\mathcal{C}}_{1,k} \\ \sum_{k=j}^T \boldsymbol{\mathcal{C}}_{2,k} \\ \mathbf{0} \end{bmatrix}, \quad (38)$$

with the dimensions of  $\boldsymbol{\mathcal{C}}_{1,k}$ ,  $\boldsymbol{\mathcal{C}}_{2,k}$  and  $\mathbf{0}$  corresponding to those of  $\mathbf{f}_j$ ,  $\mathbf{e}_j$  and  $\boldsymbol{\sigma}_j$ , respectively. The explicit expression of  $\boldsymbol{\mathcal{C}}_{1,k}$  and  $\boldsymbol{\mathcal{C}}_{2,k}$  can be obtained from the equations in [4, Appendix A].

Below, we calculate the derivative of the terms in (36) with respect to  $\mathbf{f}_j$ ,  $\mathbf{e}_j$ , and  $\boldsymbol{\sigma}_j$ , respectively.

Firstly, with respect to  $\mathbf{f}_j$ , one has

$$\nabla_{\mathbf{f}_j} \text{Tr} \boldsymbol{\lambda}_{1,k} = \mathbf{f}_j^{\top} \mathcal{M}_k^1, \quad \nabla_{\mathbf{f}_j} \text{Tr} \boldsymbol{\lambda}_{2,k} = 0, \quad \nabla_{\mathbf{f}_j} \text{Tr} \boldsymbol{\lambda}_{3,k} = 0$$

and hence

$$\begin{aligned} \nabla_{\mathbf{f}_j} \text{Tr} \boldsymbol{\lambda}_{4,k} &= \nabla_{\mathbf{f}_j} \text{Tr} \left\{ (\boldsymbol{\Sigma}_k^d)^{-1} \mathbf{B}_k^d \mathbf{F}_j \hat{\mathbf{s}}_{k|T} \mathbf{e}_j^{\top} \mathbf{B}_k^{d\top} \right\} \\ &= \nabla_{\mathbf{f}_j} \text{Tr} \left\{ (\mathbf{e}_j^{\top} \mathbf{B}_k^{d\top}) (\boldsymbol{\Sigma}_k^{d-1} \mathbf{B}_k^d \mathbf{F}_j \hat{\mathbf{s}}_{k|T}) \right\} \\ &= (\mathbf{B}_k^d \mathbf{e}_j)^{\top} \nabla_{\mathbf{f}_j} (\hat{\mathbf{s}}_{k|T}^{\top} \otimes \boldsymbol{\Sigma}_k^{d-1} \mathbf{B}_k^d) \mathbf{f}_j \\ &= [(\hat{\mathbf{s}}_{k|T} \otimes \mathbf{B}_k^d \boldsymbol{\Sigma}_k^{d-1}) (\mathbf{I} \otimes \mathbf{B}_k^d) \mathbf{e}_j]^{\top} \end{aligned}$$

and, similarly,

$$\nabla_{\mathbf{f}_j} \text{Tr} \boldsymbol{\lambda}_{5,k} = [(\hat{\mathbf{s}}_{k|T} \otimes \mathbf{B}_k^d) (\mathbf{I} \otimes \boldsymbol{\Sigma}_k^{d-1} \mathbf{B}_k^d) \mathbf{e}_j]^{\top}.$$

Here,  $\mathcal{M}_k^1 = \mathcal{M}_k^{1,0} + \mathcal{M}_k^{1,1}$  with

$$\begin{aligned} \mathcal{M}_k^{1,0} &= 2 \hat{\mathbf{s}}_{k|T} \hat{\mathbf{s}}_{k|T}^{\top} \otimes \mathbf{B}_k^d \boldsymbol{\Sigma}_k^{d-1} \mathbf{B}_k^d \\ \mathcal{M}_k^{1,1} &= 2 \hat{\mathbf{P}}_{k|T} \otimes \mathbf{B}_k^d \boldsymbol{\Sigma}_k^{d-1} \mathbf{B}_k^d. \end{aligned}$$

Secondly, with respect to  $\mathbf{e}_j$ , one has

$$\begin{aligned} \nabla_{\mathbf{e}_j} \text{Tr} \boldsymbol{\lambda}_{1,k} &= 0 \\ \nabla_{\mathbf{e}_j} \text{Tr} \boldsymbol{\lambda}_{2,k} &= \mathbf{e}_j^{\top} \mathcal{M}_k^2 \\ \nabla_{\mathbf{e}_j} \text{Tr} \boldsymbol{\lambda}_{3,k} &= 0 \\ \nabla_{\mathbf{e}_j} \text{Tr} \boldsymbol{\lambda}_{4,k} &= \mathbf{f}_j^{\top} (\mathbf{I} \otimes \mathbf{B}_k^{d\top}) (\hat{\mathbf{s}}_{k|T} \otimes \boldsymbol{\Sigma}_k^{d-1} \mathbf{B}_k^d) \\ \nabla_{\mathbf{e}_j} \text{Tr} \boldsymbol{\lambda}_{5,k} &= \mathbf{f}_j^{\top} (\mathbf{I} \otimes \boldsymbol{\Sigma}_k^{d-1} \mathbf{B}_k^d) (\hat{\mathbf{s}}_{k|T} \otimes \mathbf{B}_k^d) \end{aligned}$$

with

$$\mathcal{M}_k^2 = 2 \mathbf{I} \otimes \mathbf{B}_k^{d\top} \boldsymbol{\Sigma}_k^{d-1} \mathbf{B}_k^d.$$

From above, the equation (34) is equivalent to

$$\nabla_{\phi_j} \left\{ \mathcal{L}_j(\phi_j, \hat{\phi}^i) + \sum_{k=j+1}^T \mathcal{L}_k(\phi_{j+1}^*, \hat{\phi}^i) \right\} = \phi_j^\top \begin{bmatrix} \mathcal{M} & \mathbf{0} \\ \mathbf{0} & \mathcal{M}^2 \end{bmatrix} + \mathcal{E}^\top = \mathbf{0} \quad (39)$$

where  $\mathcal{M}^2 = \sum_{k=1}^T \mathcal{M}_k^2$ ,  $\mathcal{M} = \sum_{k=1}^T \mathcal{M}_k$ ,  $\mathcal{M}_k = \begin{bmatrix} \mathcal{M}_k^1 & \mathcal{M}_k^3 \\ \mathcal{M}_k^3^\top & \mathcal{M}_k^2 \end{bmatrix}$  with  $\mathcal{M}_k^3 = 2(\mathbf{I}_1 \otimes \mathbf{B}_k^d)^\top (\hat{\mathbf{s}}_{k|T}^\top \otimes \Sigma_k^{d-1} \mathbf{B}_k^d)$ .

What is left is to prove the existence of a unique solution  $\phi_j$  to the equation (39). It suffices to show that  $\mathcal{M} > 0$  and  $\mathcal{M}^2 > 0$ , or  $\mathcal{M}_k > 0$  and  $\mathcal{M}_k^2 > 0$ .

Since the matrix  $\mathbf{B}_k^d$  has a full column rank,  $\Sigma_k^d > 0$  and  $\hat{\mathbf{P}}_{k|T} > 0$ , one has  $\mathcal{M}_k^2 > 0$  and  $\mathcal{M}_k^{1,1} > 0$ . Next, the decomposition of the matrix  $\mathcal{M}_k$  gives

$$\mathcal{M}_k = \begin{bmatrix} \mathbf{I} & \mathcal{M}_k^3 \mathcal{M}_k^{2-1} \\ \mathbf{0} & \mathbf{I} \end{bmatrix} \begin{bmatrix} \mathcal{M}_k^1 - \mathcal{M}_k^3 \mathcal{M}_k^{2-1} \mathcal{M}_k^{3^\top} & \mathbf{0} \\ \mathbf{0} & \mathcal{M}_k^2 \end{bmatrix} \quad (40)$$

$$\begin{bmatrix} \mathbf{I} & \mathbf{0} \\ \mathcal{M}_k^{2-1} \mathcal{M}_k^{3^\top} & \mathbf{I} \end{bmatrix}. \quad (41)$$

It is noted that  $\mathcal{M}_k^{1,0} = \mathcal{M}_k^3 \mathcal{M}_k^{2-1} \mathcal{M}_k^{3^\top}$ , which implies

$$\mathcal{M}_k^1 - \mathcal{M}_k^3 \mathcal{M}_k^{2-1} \mathcal{M}_k^{3^\top} = \mathcal{M}_k^{1,1} > 0$$

and hence  $\mathcal{M}_k > 0$ . The proof is thus completed.  $\square$

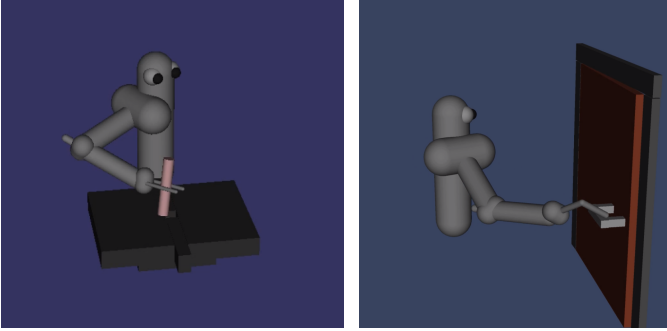


Fig. 2: MUJOCO-based simulation environment on which the DP-based stochastic optimal control algorithm is tested; **left**: A PR2 robot has the task of inserting the peg in the hole; **right**: A PR2 robot has the task of opening the door to a certain minimum angle.

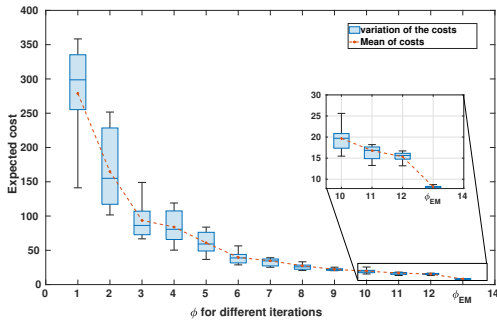


Fig. 3: Expected costs for peg in the hole task; the zoomed-in plot shows the decline in the cost when  $\phi_{12}$  is utilized to initiate the EM strategy, i.e., we used iLQG to initiate EM when I do not see much change in the previous costs.

**Theorem IV.2.** For the function  $\bar{\mathcal{L}}_k(\phi_k, \hat{\phi}^i)$  defined in (26), the following inequality

$$-\nabla_{\phi_j}^2 [\bar{\mathcal{L}}_j(\phi_j, \hat{\phi}^i) + \sum_{k=j}^T \bar{\mathcal{L}}_k(\hat{\phi}_{j+1}^*, \hat{\phi}^i)] > 0, \quad j = T, \dots, 1 \quad (42)$$

always holds for any given parameter  $\hat{\phi}^i$ ;  $\hat{\phi}_{j+1}^*$  represents the optimal parameters obtained from the backward steps of optimization as per the series of equations 31.

**Proof.** By combining the insights from Theorem IV.1 with the proof presented in [4, Theorem 3], one can directly demonstrate the theorem's validity.  $\square$

**Remark IV.2.** The two differences between the objective function in eq (32) and the objective function mentioned in [4, Section 4B] are:

- 1) For each time-varying optimization, there is the total summation across  $j^{\text{th}}$  to  $T^{\text{th}}$  time instants rather than all time instants.
- 2) A backward substitution of optimal parameters is utilized as per eq (30) that leverages optimal parameters from eq (29).

Nevertheless, the functional form which governs the optimization is essentially the same. As a result one can take very similar approach to carry out theoretical developments as per [4], [5].

## V. NEW INTERPRETATIONS/CONNECTIONS OF EM-BASED SOC WITH LEGENDRE TRANSFORM

This section aims at providing an information-theoretic perspective on the EM algorithm by highlighting its relationship with optimal control and its connections to earlier findings in the literature of stochastic control theory and dynamic games [10].

An investigation conducted by [8] has yielded a comprehensive theoretical analysis, wherein they have associated the concept of “free energy” with the formulation of optimal control. Employing the definition of free energy as a foundational premise, the authors exploit the Legendre transformation mentioned in Lemma V.1, thereby delivering a pivotal theorem that is presented in Theorem V.1. The inclusion of the following lemma serves to ensure self-containedness, enhance the overall coherence of this section and later this is used to deliver a theoretical result.

**Lemma V.1.** Consider  $(\Omega, \mathcal{F})$  to be a measurable space, where  $\Omega$  denotes the sample space and  $\mathcal{F}$  denotes a  $\sigma$ -algebra, and let  $\mathcal{P}(\Omega)$  define a probability measure on the  $\sigma$ -algebra  $\mathcal{F}$ . Consider  $\mathbb{P}, \mathbb{Q} \in \mathcal{P}(\Omega)$  and the definitions of free energy and relative entropy from Definitions 1 and 2 and under assumption  $\mathbb{Q} \ll \mathbb{P}$ , the following equality holds:

$$\left[ \frac{1}{\rho} \log \int e^{\rho \mathcal{J}(\mathcal{S}_T, \mathbb{A}_T)} d\mathbb{P} \right] = \sup_{\mathbb{Q}} [\mathbb{E}_{\mathbb{Q}} \mathcal{J}(\mathcal{S}_T, \mathbb{A}_T) - \frac{1}{\rho} D_{KL}(\mathbb{Q} \parallel \mathbb{P})], \quad (43)$$

where  $\mathcal{J}$  is a measurable function, i.e.,  $\mathcal{J}(\cdot) : \Omega \rightarrow \mathbb{R}$  and can be thought of as a cost function.<sup>3</sup>

<sup>3</sup>This cost function may be obtained as a result of controlled or uncontrolled dynamics as per [8].

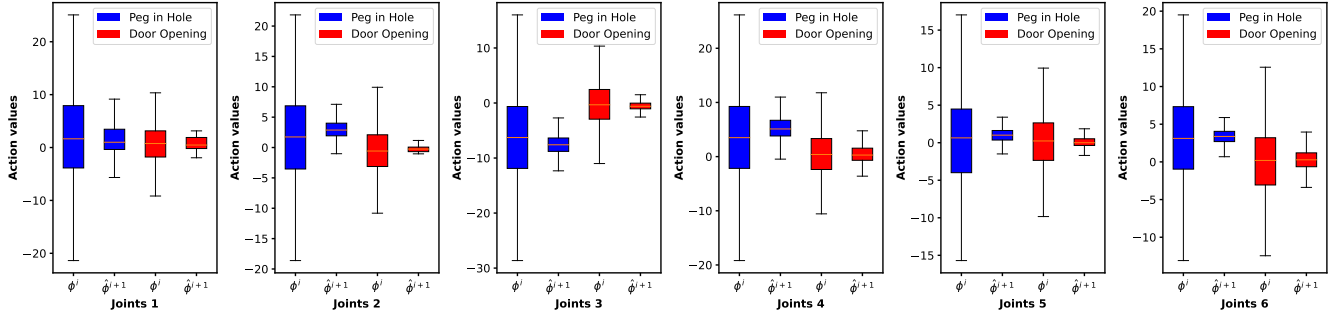


Fig. 4: The plots represents the over all variation of control actions for 40 sample paths and each sample path contains samples of horizon length  $T$  for each of the 6 DOF of PR2 robotic arm joints evaluated on two tasks corresponding to the labels of colors red and blue. The term  $\phi^i$  and  $\phi^{i+1}$  corresponds to baseline (iLQG) and improved parameters (EM) respectively.

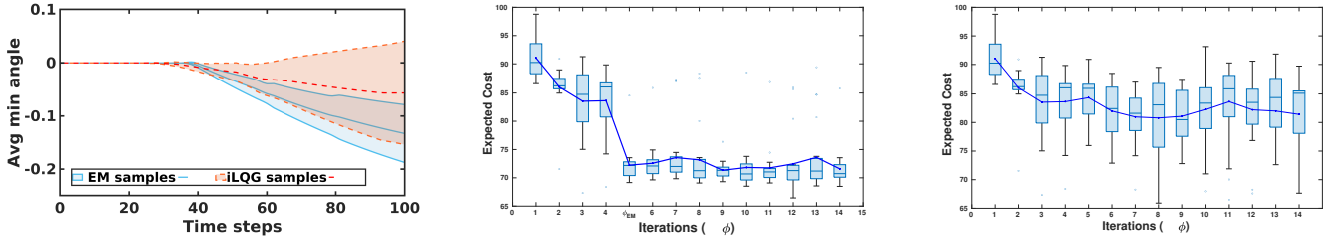


Fig. 5: **Top:** Average minimum angle in radians of the door hinge opened by the hook attached to the end effector of the PR2 robot (lower angle is better); **Bottom left:** Expected costs for door opening task based on Algorithm 1; **Bottom right:** Expected costs for door opening task for 14 iterations based on parameter obtained from iLQG.

**Proof.** One can denote the expression of expectation  $\mathbb{E}_{\mathbb{P}}$  as a function of the expectation  $\mathbb{E}_{\mathbb{Q}}$  as per Definition 2. Precisely,

$$\mathbb{E}_{\mathbb{P}} \left[ e^{\rho \mathcal{J}} \right] = \int e^{\rho \mathcal{J}} d\mathbb{P} = \int e^{\rho \mathcal{J}} \frac{d\mathbb{P}}{d\mathbb{Q}} d\mathbb{Q} \quad (44)$$

$$\Rightarrow \log \mathbb{E}_{\mathbb{P}} \left[ e^{\rho \mathcal{J}} \right] = \log \left[ \int e^{\rho \mathcal{J}} \frac{d\mathbb{P}}{d\mathbb{Q}} d\mathbb{Q} \right] \geq \int \log \left( e^{\rho \mathcal{J}} \frac{d\mathbb{P}}{d\mathbb{Q}} \right) d\mathbb{Q} \quad (45)$$

$$\Rightarrow \log \mathbb{E}_{\mathbb{P}} \left[ e^{\rho \mathcal{J}(\mathbb{S}, \mathbb{A})} \right] \geq \int \left( \rho \mathcal{J} + \log \frac{d\mathbb{P}}{d\mathbb{Q}} \right) d\mathbb{Q} = \int \rho \mathcal{J} d\mathbb{Q} - D_{\text{KL}}(\mathbb{Q} \parallel \mathbb{P}) \quad (46)$$

Eq. (45) is Jensen's inequality applied to terms of logarithm of integrals. Then, multiplying eq (46) with  $\frac{1}{\rho}$ , and applying  $\mathbb{E}_{\mathbb{Q}}(\mathcal{J}) = \int \mathcal{J} d\mathbb{Q}$ , and changing signs, one can prove eq (43).  $\square$

**Remark V.1.** Above lemma comes from [9, Theorem 1] and the value of  $\rho < 0$  describes risk sensitive attribute of the optimization. For our analysis, we will associate  $\rho < 0$  with a parameter of distribution that governs the costs/rewards observations.

The next theorem exploits the relationship between EM-based optimal control according to eq (24) and results of Lemma V.1 to provide a novel interpretation.

**Theorem V.1.** Assuming  $\rho = -(\lambda - 1)$ , where  $\lambda$  is a parameter as per Assumption III.1, the EM-based optimal control approach is a special case of infimum operation on the free energy (as per Definition 1) i.e.,

$$\inf_{\hat{\mathbb{A}}_T} \left[ \log \int e^{\rho \sum_{k=1}^T Y_k(\mathbf{s}_k, \mathbf{a}_k)} \right] = \sup_{\phi} \mathcal{L}(\phi, \hat{\phi}^i) \quad (47)$$

**Proof.** Exploiting Lemma V.1 and substituting,  $\mathbb{P} = p_{\hat{\phi}^i}(\mathbb{S}_{T+1} \mid \mathbb{Y}_T)$  and  $\mathbb{Q} = \tilde{p}(s_k)$  and utilizing Definition 1, i.e.,  $\mathcal{E} \triangleq \mathbb{E}(\mathcal{J}(\mathbb{S}_T, \mathbb{A}_T)) = \log \int e^{\rho \mathcal{J}(\mathbb{S}_T, \mathbb{A}_T)}$ , where

$\mathcal{J}(\mathbb{S}_T, \mathbb{A}_T) \triangleq \sum_{k=1}^T Y_k(\mathbf{s}_k, \mathbf{a}_k)$ , thus upon expansion of the free energy term and exploiting the Jensen's inequality,

$$\log \int e^{\rho \sum_{k=1}^T Y_k(\mathbf{s}_k, \mathbf{a}_k)} \quad (48)$$

$$\geq \int \log \left( e^{\rho \mathcal{J}(\cdot)} \frac{dp_{\hat{\phi}^i}(\mathbb{S}_{T+1} \mid \mathbb{Y}_T)}{d\tilde{p}(\mathbb{S}_T)} \right) d\tilde{p}(\mathbb{S}_T) \quad (49)$$

$$\begin{aligned} &\Rightarrow \log \int e^{\rho \sum_{k=1}^T Y_k(\mathbf{s}_k, \mathbf{a}_k)} \\ &\geq \mathbb{E}_{\tilde{p}(s_k)} \left[ \log \frac{dp_{\hat{\phi}^i}(\mathbb{S}_{T+1} \mid \mathbb{Y}_T)}{d\tilde{p}(\mathbb{S}_T)} + \rho \mathcal{J}(\mathbb{S}_T, \mathbb{A}_T) \right] \quad (50) \end{aligned}$$

$$\begin{aligned} &\Rightarrow \log \int e^{\rho \sum_{k=1}^T Y_k(\mathbf{s}_k, \mathbf{a}_k)} \\ &\geq -D_{\text{KL}}(\tilde{p}(s_k) \parallel p_{\hat{\phi}^i}(\mathbb{S}_{T+1} \mid \mathbb{Y}_T)) + \mathbb{E}_{\tilde{p}(s_k)}[\rho \mathcal{J}(\mathbb{S}_T, \mathbb{A}_T)] \quad (51) \end{aligned}$$

$$\Rightarrow \mathcal{E}(\cdot) = \sup_{d\mathbb{Q}} \left[ -D_{\text{KL}}(\tilde{p}(s_k) \parallel p_{\hat{\phi}^i}(\cdot)) + \mathbb{E}_{\tilde{p}(s_k)} \rho \mathcal{J}(\cdot) \right], \quad (52)$$

Essentially, one can define the minimization problem as:

$$\log \int e^{\rho \sum_{k=1}^T Y_k(\mathbf{s}_k, \mathbf{a}_k)} \quad (53)$$

$$= \sup_{d\mathbb{Q}} \left[ -D_{\text{KL}}(\mathbb{Q} \parallel p_{\hat{\phi}^i}(\cdot)) + \mathbb{E}_{\tilde{p}(s_k)} \rho \mathcal{J}(\cdot) \right] \quad (54)$$

$$\Rightarrow \mathcal{E}(\cdot) = \sup_{d\mathbb{Q}} \left[ -D_{\text{KL}}(\mathbb{Q} \parallel p_{\hat{\phi}^i}(\cdot)) + \mathbb{E}_{\tilde{p}(s_k)} \rho \mathcal{J}(\cdot) \right], \quad (55)$$

where the  $(\cdot)$  is used for shortness of expression. The eq. (55) is of a very similar structure as that of eq. (66), which shows a special case where the free energy definition can be reduced to E-step for optimal policy. Further, assuming  $\rho = -(\lambda - 1)$ , one can see,

$$\mathcal{E}(\cdot) = \inf_{d\mathbb{Q}} \left[ D_{\text{KL}}(\tilde{p}(s_k) \parallel p_{\hat{\phi}^i}(\mathbb{S}_{T+1} \mid \mathbb{Y}_T)) + \mathbb{E}_{\tilde{p}(s_k)} (\lambda - 1) \mathcal{J}(\cdot) \right]. \quad (56)$$

If  $\tilde{p}(s_k) = p_{\hat{\phi}^i}(S_{T+1}|\mathbb{Y}_T)$ , then, one can minimize the free energy  $\mathcal{E}(\cdot)$  on set of control action  $\{\mathbf{a}_1, \dots, \mathbf{a}_T\}$ . Without loss of generality, the set of control actions  $\{\mathbf{a}_1, \dots, \mathbf{a}_T\}$  can be represented in terms of parameters  $\phi$ , therefore,

$$\inf_{\mathbf{a}_1, \dots, \mathbf{a}_T} \mathcal{E}(\cdot) = \inf_{\mathbf{a}_1, \dots, \mathbf{a}_T} \left[ \inf_{d\mathbb{Q}} [\mathbb{E}_{\mathbb{Q}}(\lambda - 1) \mathcal{J}(\cdot)] \right] \quad (57)$$

$$= \sup_{\phi} \underbrace{\inf_{d\mathbb{Q}} [l(\phi, \mathbb{Q})]}_{\text{E-step of EM-SOC}} \quad (58)$$

$$= \sup_{\phi} \underbrace{\mathcal{L}(\phi, \hat{\phi}^i)}_{\text{M-step of EM-SOC}}. \quad (59)$$

The eq. (59) is a direct result of infimum operation over a set of  $\phi$  on eq. (67).  $\square$

**Remark V.2.** The parameter  $\rho$  plays the similar role as that of  $-(\lambda - 1)$  and this theorem establishes that EM-based optimal control according to eq. (24) is a special case of minimization of free energy-relative entropy. Also, it can be noted that the expectation operator is taken with respect to some p.d.f. of the states which evolve according to the controlled dynamics (as per the linear Gaussian model (6)), whereas [8, Section 3] deals both with controlled and uncontrolled dynamics. Nevertheless, this specialised reduction of optimization operations under some assumptions can be reduced to be equivalent to optimization. This also provides novel interpretation of the duality between the already existing information-theoretic-based min-max SOC approach (from Eq. (43)) and that of the proposed objective function (according to Eq. (24))

## VI. EXPERIMENTAL RESULTS

We evaluated our method on simulations conducted on a platform known as MUJOCO; please see [6] for details of the kinematics and dynamics of the models embedded in the framework which utilizes a system of rigid links with noisy motors at the joints. Inside the MUJOCO framework we used a model of a PR2 robot to try to address two tasks as mentioned below:

- 1) Door opening task: This task requires opening a door with a 6 degree of freedom (DOF) 3D robotic arm. In this task the arm must grasp the handle and then pull the door to a target angle, which is challenging for model-based methods due to the complicated contact dynamics between the hand and the handle. A contact needs to be established before the door can be opened. The cost function utilized is a weighted combination of the distance of the end effector to the door handle with that of the angle of the door. The right sub-figure of Fig 2 shows an instance of the simulation.
- 2) Peg in a hole task: This particular task requires inserting the peg which is attached to the end effector of the PR2 robot in a hole which is created in a board placed in front of PR2 manipulator. The left sub-figure of Fig 2 depicts an instance of the task of inserting the peg in the hole.

We consider sensor noise  $\boldsymbol{\epsilon}_k^s$  to be Gaussian in our experiments, i.e.,

$$\mathbf{s}_k = \mathbf{x}_k + \boldsymbol{\epsilon}_k^s, \quad \boldsymbol{\epsilon}_k^s \sim \mathcal{N}(0, \rho^2 \mathbf{I}_{n_s}), \quad (60)$$

where  $\mathbf{x}_k$  is the real state. The sensor noise  $\boldsymbol{\epsilon}_k^s$  is indirectly propagated into the design of control action  $\mathbf{a}_k$  that forms the real input to the system. For conducting the experiments I utilized  $\rho^2 = 0.1$  and followed the steps as mentioned in Algorithm 1.

**Cost:** For the door opening task, the mean $\pm$ std-dev of the expected real costs  $\sum_{l=1}^T Y_l(s_l, \mathbf{a}_l)$  for 14 iterations are depicted in the bottom two sub-plots of Fig. 5. The datasets take into account 20 samples;

the bottom left utilizes Algorithm 1 whereas the bottom right is when a particular baseline, i.e., iLQG, is used for 14 continuous iterations. The noise parameter was set as  $\rho^2 = 0.1$ . The continuous line in the bottom sub-plots in blue represents the mean of the cost for a particular iteration and the box plots represent a variation of the costs for iterations. The bottom right plot provides expected costs for a particular baseline i.e., iLQG for 14 iterations and the bottom left plot shows the course of expected costs if on fourth iteration EM-based parameters  $\hat{\phi}^{i+1}$  is utilized and then the iLQG is repeated from the 6<sup>th</sup> iterations. A very interesting result can be seen as compared to running full iLQG iterations for 14 iterations, without the intervention of EM-based optimization. The top plot shows the average min angle in radians of the door hinge to which the door is pulled by the hook attached to the end effector. It can be clearly seen that the EM samples of the door provide a better minimum angle of opening compared to the baseline.

For the peg in the hole task, the mean $\pm$ std-dev of the expected real costs  $\sum_{l=1}^T Y_l(s_l, \mathbf{a}_l)$  for 13 iterations for this task is shown in 3. I utilized  $\phi^{12}$  as an initialization for obtaining  $\hat{\phi}^{i+1}$  based on (32)

**Trajectories:** We compare the true state trajectories, i.e.,  $\{\mathbf{x}_1, \dots, \mathbf{x}_T\}$  produced on the real platform excited by the control actions with the parameters obtained through repeated EM iterations. In this experiment, iLQG was used as the baseline. We performed 20 experiments and each experiment ran for 14 subsequent iterations. The mean $\pm$ std-dev of the trajectories  $[x_k, y_k, z_k]$ ,  $k = 1, \dots, T$ , for the position of the end-effector is illustrated in Fig. 6 and Fig. 7 for the tasks of peg in the hole and door opening, respectively. It can be observed that evolution of the state trajectories demonstrates better performance achieved by EM iterations in terms of less stochasticity in the states. In particular, there is a high variance in the dashed trajectories compared to the solid lines. The advantage gained by the EM iterations can be explained by the less deviation caused by noise. It has been shown that the exploitation functionality of the EM approach can effectively reduce the stochasticity in control policies. Fig. 7 shows the evolution of the end effector position, i.e.,  $[x, y, z]$  states of the hook. All plots are divided into solid and dashed lines and the respective deviation is from a set of 20 experiments conducted from the same initial condition with a total horizon of the experiment being  $T = 100$ . The superiority of the DPSOC-EM is noticeable in terms of the uncertainty reduction by the generated optimal control estimates. A similar profile, can be seen resulting from Fig 6, where each plot exhibits two variables corresponding to the top and bottom end of the peg; e.g., the top plot of Fig 6 shows the  $x$  position of the two ends of the peg, where the solid lines and respective deviations (in shade) correspond to the EM parameter estimates and the dash lines and the deviations correspond to the iLQG parameter estimates. This figure show the temporal evolution of states for a total time  $T = 70$ .

**Performance comparison in the video:** For the two tasks, the simulation video for the comparison of iLQG and EM-based optimal control can be visualized via gif file that can be found in the following [Github](#) link. In the above shown video links, the left video corresponds to the baseline policy and the right one corresponds to the parameters derived as a result of the approach mentioned in this chapter. It can be visualised in the simulation (for both tasks) that the stochasticity of end effector is evident from the jittery nature of the joints of the PR2 robot when its trying to accomplish the two tasks.

**Exploitation efficiency in control actions:** Fig 4 shows 6 plots each corresponding to the control actions of joints of the PR2 robot for the door opening task as well as the peg in the hole tasks depicted in Fig 2. Referring to Fig 4, one can see that each sub-plot contains 4 box plots with two different color. Each color shade

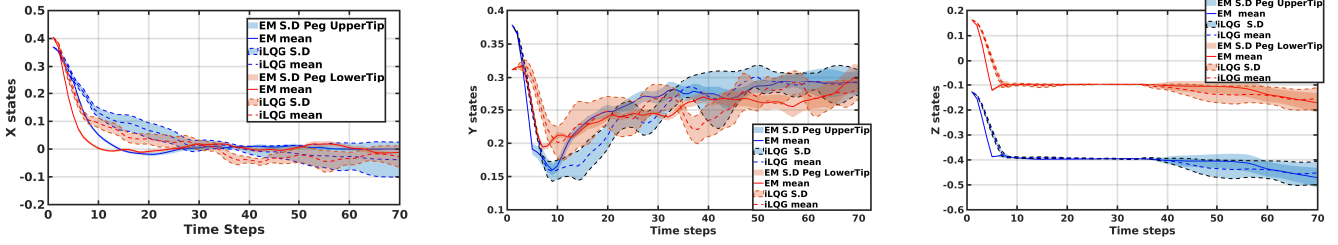


Fig. 6: Three states i.e.,  $[x, y, z]$  positions of the peg which is connected to the end-effector of PR2 robot. Each plot of this figure is divided into two coloured plots that shows the mean and variance of the state trajectories. The dashed lines represents iLQG trajectories and solid lines represents that of parameters obtained from eq (32).

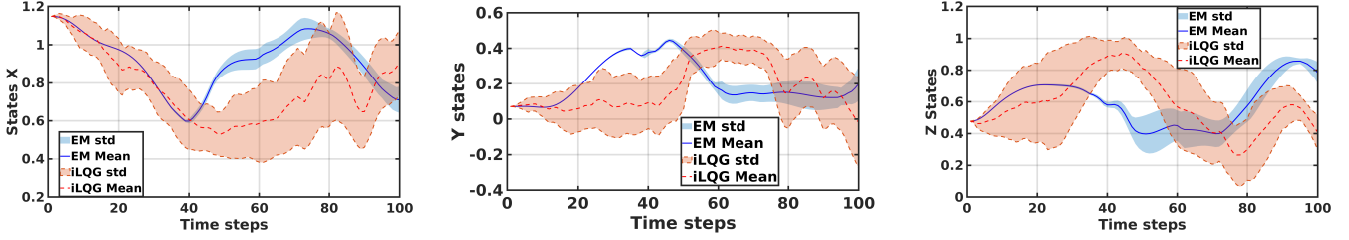


Fig. 7: Evolution of three states corresponding to position  $[x, y, z]$  of the door-opening task, where the positions represent that of the hook which is connected to the end-effector. Each plot of this figure is divided into two coloured plots that shows the mean and variance of the state trajectories. The dashed lines represent  $\phi$  obtained from iLQG and solid lines represent trajectories obtained from  $\phi^*$  of eq (32).

is specific to each task, i.e., blue corresponds to Peg in hole task and red corresponds to door opening task. Each box plot shows a variation of actions,  $a_k^n \forall k \in \{1, \dots, T\}$  and  $\forall n \in \{1, \dots, 40\}$ , where  $n$  denotes samples/trajectories. Each color has two pairs of results,  $\phi^i$  and  $\hat{\phi}^{i+1}$  denoting the baseline iLQG and EM parameters respectively. One can notice that the superiority in the proposed optimization approach is evident from the lesser deviations in terms of control action values. The observed improvement in control actions is attributed to the exploitation mechanism in the DPSOC-EM approach that significantly reduces the stochasticity (variation) in the control policies over multiple samples over the total horizon.

The simulations for Step 1, 2 and 5 were performed using the 64-bit Ubuntu 16.04 OS on Dell Alienware 15 R2 of Intel Core i7-6700HQ CPU @ 2.60GHz. The simulations for Step 3 and 4 were conducted using multiple 2.6 GHz Intel Xeon Broadwell (E5-2697A v4) processors on the high performance computing (HPC) grid located at The University of Newcastle.

## VII. CONCLUSION

This paper focuses on two major parts; a) provides an alternate version of approximate DDP i.e., DPSOC-EM, b) delivers novel connections between information theory and stochastic control dualities with optimisation of mixture likelihood. The new approximate control paradigm has a similar analytical architecture as that mentioned in the paper [4, Section 4]. As a result of this structure, the analytical guarantees of surrogate function holds. It has also been shown empirically to generate superior estimates as compared to baselines, e.g., the superiority of the DPSOC-EM is noticeable in terms of the uncertainty reduction (both in the control action and the states) by the generated estimates and also the reduction of the overall cost function.

## APPENDIX

### A. Some EM Lemmas

**Lemma A.1.** Consider  $L_\phi(\mathbb{Y}_T)$  and  $\mathcal{L}(\phi, \hat{\phi}^i)$  defined in (22) and (23), respectively, with  $\hat{\phi}^i$  a known parameter estimate. Let

$$l(\phi, \tilde{p}(\mathbb{S}_{T+1})) = \mathbb{E}_{\tilde{p}(\mathbb{S}_{T+1})} \log \frac{p_\phi(\mathbb{S}_{T+1}, \mathbb{Y}_T)}{\tilde{p}(\mathbb{S}_{T+1})} \quad (61)$$

for any distribution  $\tilde{p}(\mathbb{S}_{T+1})$ . One has

$$L_\phi(\mathbb{Y}_T) \geq l(\phi, \tilde{p}(\mathbb{S}_{T+1})),$$

that is,  $l(\phi, \tilde{p}(\mathbb{S}_{T+1}))$  is a lower bound of  $L_\phi(\mathbb{Y}_T)$ . Moreover, let

$$\tilde{p}(\mathbb{S}_{T+1}) = p_{\hat{\phi}^i}(\mathbb{S}_{T+1} | \mathbb{Y}_T), \quad (62)$$

and denote

$$l(\phi, \hat{\phi}^i) = l(\phi, p_{\hat{\phi}^i}(\mathbb{S}_{T+1} | \mathbb{Y}_T)). \quad (63)$$

One has

$$\hat{\phi}^{i*} = \arg \max_{\phi} l(\phi, \hat{\phi}^i) = \arg \max_{\phi} \mathcal{L}(\phi, \hat{\phi}^i). \quad (64)$$

**Proof.** One can start by expanding  $L_\phi(\mathbb{Y}_T)$  as follows

$$\begin{aligned} L_\phi(\mathbb{Y}_T) &= \log p_\phi(\mathbb{Y}_T) \\ &= \log \int p_\phi(\mathbb{Y}_T, \mathbb{S}_{T+1}) d\mathbb{S}_{T+1} \\ &= \log \int \tilde{p}(\mathbb{S}_{T+1}) \frac{p_\phi(\mathbb{S}_{T+1}, \mathbb{Y}_T)}{\tilde{p}(\mathbb{S}_{T+1})} d\mathbb{S}_{T+1} \\ &\geq \int \tilde{p}(\mathbb{S}_{T+1}) \log \frac{p_\phi(\mathbb{S}_{T+1}, \mathbb{Y}_T)}{\tilde{p}(\mathbb{S}_{T+1})} d\mathbb{S}_{T+1} \\ &= \mathbb{E}_{\tilde{p}(\mathbb{S}_{T+1})} \log \frac{p_\phi(\mathbb{S}_{T+1}, \mathbb{Y}_T)}{\tilde{p}(\mathbb{S}_{T+1})} \\ &= l(\phi, \tilde{p}(\mathbb{S}_{T+1})), \end{aligned} \quad (65)$$

which holds for any distribution  $\tilde{p}(\mathbb{S}_{T+1})$ . Nevertheless, one requires  $\tilde{p}(\mathbb{S}_{T+1})$  to deliver an optimal bound such that, at a known value

(current estimate) of  $\phi$ , the bound  $l(\phi, \tilde{p}(\mathbb{S}_{T+1}))$  touches  $L_\phi(\mathbb{Y}_T)$ . We can further expand the lower bound  $l(\phi, \tilde{p}(\mathbb{S}_{T+1}))$  as follows,

$$\begin{aligned}
& l(\phi, \tilde{p}(\mathbb{S}_{T+1})) \\
&= \int \tilde{p}(\mathbb{S}_{T+1}) \log \frac{p_\phi(\mathbb{S}_{T+1}, \mathbb{Y}_T)}{\tilde{p}(\mathbb{S}_{T+1})} d\mathbb{S}_{T+1} \\
&= \int \tilde{p}(\mathbb{S}_{T+1}) \log \frac{p_\phi(\mathbb{S}_{T+1}|\mathbb{Y}_T)p_\phi(\mathbb{Y}_T)}{\tilde{p}(\mathbb{S}_{T+1})} d\mathbb{S}_{T+1} \\
&= \int \tilde{p}(\mathbb{S}_{T+1}) \log \frac{p_\phi(\mathbb{S}_{T+1}|\mathbb{Y}_T)}{\tilde{p}(\mathbb{S}_{T+1})} d\mathbb{S}_{T+1} \\
&\quad + \int \tilde{p}(\mathbb{S}_{T+1}) \log p_\phi(\mathbb{Y}_T) d\mathbb{S}_{T+1} \\
&= \mathbb{E}_{\tilde{p}(\mathbb{S}_{T+1})} \log \frac{p_\phi(\mathbb{S}_{T+1}|\mathbb{Y}_T)}{\tilde{p}(\mathbb{S}_{T+1})} + \mathbb{E}_{\tilde{p}(\mathbb{S}_{T+1})} \log p_\phi(\mathbb{Y}_T) \\
&= -\mathbf{D}_{\text{KL}}(\tilde{p}(\mathbb{S}_{T+1})||p_\phi(\mathbb{S}_{T+1}|\mathbb{Y}_T)) + \log p_\phi(\mathbb{Y}_T). \quad (66)
\end{aligned}$$

It indicates that the tight optimal distribution (62) is clearly is a consequence of  $\mathbf{D}_{\text{KL}}(\cdot) = 0$  as  $\mathbf{D}_{\text{KL}} \geq 0$ . So, the selection (62) basically utilizes the known estimate  $\hat{\phi}^i$  to solve for  $\tilde{p}(\mathbb{S}_{T+1})$ . This step of solving for optimal distribution of  $\tilde{p}(\mathbb{S}_{T+1})$  is called the E-step.

With (62), we can denote (63), which is re-calculated below, noting (23) and (61),

$$\begin{aligned}
l(\phi, \hat{\phi}^i) &= \mathbb{E}_{\hat{\phi}^i}(\log p_\phi(\mathbb{S}_{T+1}, \mathbb{Y}_T)|\mathbb{Y}_T) \\
&\quad - \mathbb{E}_{p_{\hat{\phi}^i}(\mathbb{S}_{T+1}|\mathbb{Y}_T)}(\log p_{\hat{\phi}^i}(\mathbb{S}_{T+1}|\mathbb{Y}_T)) \\
&= \mathcal{L}(\phi, \hat{\phi}^i) - \mathbb{E}_{p_{\hat{\phi}^i}(\mathbb{S}_{T+1}|\mathbb{Y}_T)}(\log p_{\hat{\phi}^i}(\mathbb{S}_{T+1}|\mathbb{Y}_T)). \quad (67)
\end{aligned}$$

Maximizing  $l(\phi, \hat{\phi}^i)$  with respect to  $\phi$  is exactly equivalent to maximizing  $\mathcal{L}(\phi, \hat{\phi}^i)$  as the second term on the RHS of (67) is independent on  $\phi$ , that is, (64) is proved. In particular, the subsequent step for maximizing  $\mathcal{L}(\phi, \hat{\phi}^i)$  is called the M-step.  $\square$

**Lemma A.2.** Suppose the parameter  $\hat{\phi}^{i+1}$  is produced in an iteration, one that

$$L_{\hat{\phi}^{i+1}}(\mathbb{Y}_T) - L_{\hat{\phi}^i}(\mathbb{Y}_T) \geq \mathcal{L}(\hat{\phi}^{i+1}, \hat{\phi}^i) - \mathcal{L}(\hat{\phi}^i, \hat{\phi}^i) \quad (68)$$

where the equality holds if  $p_{\hat{\phi}^{i+1}}(\mathbb{S}_{T+1}|\mathbb{Y}_T) = p_{\hat{\phi}^i}(\mathbb{S}_{T+1}|\mathbb{Y}_T)$ .

**Proof.** The proof is the fundamental development of [31] and other details of assumptions and convergence can be found in [32], [33]. One can expand  $\mathcal{L}(\phi, \hat{\phi}^i)$  in a straightforward manner, using (23),

$$\begin{aligned}
\mathcal{L}(\phi, \hat{\phi}^i) &= \mathbb{E}_{\hat{\phi}^i}(\log p_\phi(\mathbb{S}_{T+1}, \mathbb{Y}_T)|\mathbb{Y}_T) \\
&= \mathbb{E}_{p_{\hat{\phi}^i}(\mathbb{S}_{T+1}|\mathbb{Y}_T)}(\log p_\phi(\mathbb{S}_{T+1}|\mathbb{Y}_T)) \\
&\quad + \mathbb{E}_{p_{\hat{\phi}^i}(\mathbb{S}_{T+1}|\mathbb{Y}_T)}(\log p_\phi(\mathbb{Y}_T)) \\
&= \mathbb{E}_{p_{\hat{\phi}^i}(\mathbb{S}_{T+1}|\mathbb{Y}_T)}(\log p_\phi(\mathbb{S}_{T+1}|\mathbb{Y}_T)) + \log p_\phi(\mathbb{Y}_T).
\end{aligned}$$

Therefore,

$$\begin{aligned}
& \mathcal{L}(\phi, \hat{\phi}^i) - \mathcal{L}(\hat{\phi}^i, \hat{\phi}^i) \\
&= \mathbb{E}_{p_{\hat{\phi}^i}(\mathbb{S}_{T+1}|\mathbb{Y}_T)} \log \frac{p_\phi(\mathbb{S}_{T+1}|\mathbb{Y}_T)}{p_{\hat{\phi}^i}(\mathbb{S}_{T+1}|\mathbb{Y}_T)} + L_\phi(\mathbb{Y}_T) - L_{\hat{\phi}^i}(\mathbb{Y}_T) \\
&= -\mathbf{D}_{\text{KL}}(p_{\hat{\phi}^i}(\mathbb{S}_{T+1}|\mathbb{Y}_T)||p_\phi(\mathbb{S}_{T+1}|\mathbb{Y}_T)) + L_\phi(\mathbb{Y}_T) - L_{\hat{\phi}^i}(\mathbb{Y}_T) \\
&\leq L_\phi(\mathbb{Y}_T) - L_{\hat{\phi}^i}(\mathbb{Y}_T),
\end{aligned}$$

which verifies (68) with  $\phi = \hat{\phi}^{i+1}$ .  $\square$

## REFERENCES

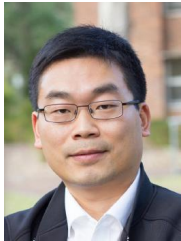
- [1] E. Todorov and W. Li, "A generalized iterative lqg method for locally-optimal feedback control of constrained nonlinear stochastic systems," in *Proceedings of the 2005, American Control Conference*. IEEE, 2005, pp. 300–306.
- [2] M. Toussaint, "Robot trajectory optimization using approximate inference," in *Proceedings of the 26th annual international conference on machine learning*. ACM, 2009, pp. 1049–1056.
- [3] J. Schulman, J. Ho, A. Lee, I. Awwal, H. Bradlow, and P. Abbeel, "Finding locally optimal, collision-free trajectories with sequential convex optimization," in *Proc. Robotics: Science and Systems*, 2013.
- [4] P. Mallick and Z. Chen, "Stochastic optimal control for multivariable dynamical systems using expectation maximization," *IEEE Transactions on Neural Networks and Learning Systems*, 2022.
- [5] P. Mallick, Z. Chen, and M. Zamani, "Reinforcement learning using expectation maximization based guided policy search for stochastic dynamics," *Neurocomputing*, vol. 484, pp. 79–88, 2022.
- [6] E. Todorov, T. Erez, and Y. Tassa, "Mujoco: A physics engine for model-based control," in *Intelligent Robots and Systems (IROS), 2012 IEEE/RSJ International Conference on*. IEEE, 2012, pp. 5026–5033.
- [7] Y. Chebotar, K. Hausman, M. Zhang, G. Sukhatme, S. Schaal, and S. Levine, "Combining model-based and model-free updates for trajectory-centric reinforcement learning," in *Proceedings of the 34th International Conference on Machine Learning-Volume 70*. JMLR. org, 2017, pp. 703–711.
- [8] E. A. Theodorou and E. Todorov, "Relative entropy and free energy dualities: Connections to path integral and kl control," in *51st IEEE Conference on Decision and Control (CDC)*. IEEE, 2012, pp. 1466–1473.
- [9] E. A. Theodorou, "Nonlinear stochastic control and information theoretic dualities: Connections, interdependencies and thermodynamic interpretations," *Entropy*, vol. 17, no. 5, pp. 3352–3375, 2015.
- [10] P. Dai Pra, L. Meneghini, and W. J. Runggaldier, "Connections between stochastic control and dynamic games," *Mathematics of Control, Signals and Systems*, vol. 9, no. 4, pp. 303–326, 1996.
- [11] P. Billingsley, *Probability and measure*. John Wiley & Sons, 2008.
- [12] R. F. Stengel, *Optimal Control and Estimation*. Courier Corporation, 1994.
- [13] C. H. Papadimitriou and J. N. Tsitsiklis, "The complexity of markov decision processes," *Mathematics of Operations Research*, vol. 12, no. 3, pp. 441–450, 1987. [Online]. Available: <http://www.jstor.org/stable/3689975>
- [14] R. Platt Jr, R. Tedrake, L. Kaelbling, and T. Lozano-Perez, "Belief space planning assuming maximum likelihood observations," 2010.
- [15] W. Li and E. Todorov, "Iterative linear quadratic regulator design for nonlinear biological movement systems," in *ICINCO (1)*, 2004, pp. 222–229.
- [16] Y. Tassa, T. Erez, and E. Todorov, "Synthesis and stabilization of complex behaviors through online trajectory optimization," in *Intelligent Robots and Systems (IROS), 2012 IEEE/RSJ International Conference on*. IEEE, 2012, pp. 4906–4913.
- [17] S. Levine, "Motor skill learning with local trajectory methods," Ph.D. dissertation, Stanford University, 2014.
- [18] B. D. Ziebart, J. A. Bagnell, and A. K. Dey, "Modeling interaction via the principle of maximum causal entropy," in *International Conference on Machine Learning*, 2010.
- [19] H. J. Kappen, V. Gómez, and M. Opper, "Optimal control as a graphical model inference problem," *Machine Learning*, vol. 87, no. 2, pp. 159–182, 2012.
- [20] E. Todorov, "Linearly-solvable markov decision problems," in *Advances in Neural Information Processing Systems*, 2007, pp. 1369–1376.
- [21] M. L. Littman, "Memoryless policies: Theoretical limitations and practical results," in *From Animals to Animats 3: Proceedings of the third international conference on simulation of adaptive behavior*, vol. 3. Cambridge, MA, 1994, p. 238.
- [22] C. Lusena, J. Goldsmith, and M. Mundhenk, "Nonapproximability results for partially observable markov decision processes," *Journal of Artificial Intelligence Research*, vol. 14, pp. 83–103, 2001.
- [23] S. Levine, C. Finn, T. Darrell, and P. Abbeel, "End-to-end training of deep visuomotor policies," *The Journal of Machine Learning Research*, vol. 17, no. 1, pp. 1334–1373, 2016.
- [24] C. M. Bishop, *Pattern Recognition and Machine Learning*. springer, 2006.
- [25] G. F. Cooper, "A method for using belief networks as influence diagrams," *arXiv preprint arXiv:1304.2346*, 2013.

- [26] P. Dayan and G. E. Hinton, "Using expectation-maximization for reinforcement learning," *Neural Computation*, vol. 9, no. 2, pp. 271–278, 1997.
- [27] M. Norouzi, S. Bengio, N. Jaitly, M. Schuster, Y. Wu, D. Schuurmans *et al.*, "Reward augmented maximum likelihood for neural structured prediction," in *Advances In Neural Information Processing Systems*, 2016, pp. 1723–1731.
- [28] S. Levine and P. Abbeel, "Learning neural network policies with guided policy search under unknown dynamics," in *Advances in Neural Information Processing Systems*, 2014, pp. 1071–1079.
- [29] D. P. Bertsekas, *Dynamic Programming and Optimal Control*. Athena scientific Belmont, MA, 1995, vol. 1, no. 2.
- [30] Y. Chebotar, M. Kalakrishnan, A. Yahya, A. Li, S. Schaal, and S. Levine, "Path integral guided policy search," in *2017 IEEE international conference on robotics and automation (ICRA)*. IEEE, 2017, pp. 3381–3388.
- [31] A. P. Dempster, N. M. Laird, and D. B. Rubin, "Maximum likelihood from incomplete data via the em algorithm," *Journal of the Royal Statistical Society. Series B*, pp. 1–38, 1977.
- [32] G. McLachlan and T. Krishnan, *The EM Algorithm and Extensions*. John Wiley & Sons, 2007, vol. 382.
- [33] C. J. Wu *et al.*, "On the convergence properties of the em algorithm," *The Annals of Statistics*, vol. 11, no. 1, pp. 95–103, 1983.



**Prakash Mallick** holds a B.Tech, M.Eng, and Ph.D. from the National Institute of Technology, Rourkela, India, University of Melbourne, Australia, and University of Newcastle, Australia, respectively (awarded in 2012, 2017, and 2023). With extensive industrial research and development experience, including three years as an electrical engineer in Coal India Limited and one year in quantitative research at Ardea Investment Management, he currently serves as a postdoctoral research fellow at the Australian Institute of Machine Learning (AIML) funded by

Defence Science and Technology Group (DSTG), Adelaide.



**Zhiyong Chen** received the B.E. degree from the University of Science and Technology of China, and the M.Phil. and Ph.D. degrees from the Chinese University of Hong Kong, in 2000, 2002 and 2005, respectively. He worked as a Research Associate at the University of Virginia during 2005-2006. He joined the University of Newcastle, Australia, in 2006, where he is currently a Professor. He was also a Changjiang Chair Professor with Central South University, Changsha, China. His research interests include non-linear systems and control, biological

systems, and multi-agent systems. He is/was an associate editor of *Automatica*, *IEEE Transactions on Automatic Control* and *IEEE Transactions on Cybernetics*.